Geophysical Research Letters

RESEARCH LETTER
10.1029/2020GL089039

Intermittent Slip Along the Alto Tiberina Low-Angle Normal Fault in Central Italy

A. Vuan[1], P. Brondi[1], M. Sugan[1], L. Chiaraluce[2], R. Di Stefano[2], and M. Michele[2]

[1]National Institute of Oceanography and Applied Geophysics-OGS, Trieste, Italy, [2]National Institute of Geophysics and Volcanology-INGV, Roma, Italy

Key Points:
- By template matching we obtain a fivefold increase of the detected events on the Alto Tiberina fault highlighting clusters and swarms
- From 2010 to 2014, microseismicity is released at variable intermittent rates often interacting with shallow, moderate seismic sequences
- In 2013, the rise in seismicity suggests an active role of the Alto Tiberina fault during aseismic slip associated with a shallow sequence

Supporting Information:
- Supporting Information S1
- Figure S1

Correspondence to:
A. Vuan,
avuan@inogs.it

Citation:
Vuan, A., Brondi, P., Sugan, M., Chiaraluce, L., Di Stefano, R., & Michele, M. (2020). Intermittent slip along the Alto Tiberina low-angle normal fault in central Italy. *Geophysical Research Letters*, *47*, e2020GL089039. https://doi.org/10.1029/2020GL089039

Received 26 MAY 2020
Accepted 14 AUG 2020
Accepted article online 21 AUG 2020

Abstract The Alto Tiberina normal fault (ATF) in central Italy is a 50-km-long crustal structure that dips at a low angle (15–20°). Events on the fault plane are about 10 times less frequent than those located in its shallower syn- and antithetic hanging-wall splays. To enhance ATF catalog and achieve a better understanding of the degree of coupling in the fault system, we apply a template matching technique in the 2010–2014 time window. We augment by a factor 5 the detections and decrease the completeness magnitude to negative values. Contrary to what previously observed on ATF, we highlight intermittent seismic activity and long-lasting clusters interacting with sequences on the shallower splays. One of these episodes of prolonged seismic activity, detected at the end of 2013 on a 30-km-long ATF segment, suggest the ATF active role during an aseismic transient unraveled by geodetic data.

Plain Language Summary Small magnitude events have regularly shaken the 50-km-long Alto Tiberina low-angle normal fault (ATF) in central Italy. Above it, few kilometers long syn- and antithetic higher-angle normal faults were active with many moderate seismic sequences and 10 times more events than ATF between 2010 and 2014. To better understand the fault system interaction, we apply a technique for finding events which match predefined templates to improve the ATF seismic catalog. The results indicate that productive sequences in the shallower high-angle faults often hamper the detection of microseismicity along with the ATF and that events are released at intermittent rates. Moreover, the seismic activity is mainly organized in clusters of small earthquakes lasting days or months with no identifiable mainshock. These clusters span a 30-km-long segment and coincide with transient deformation recorded at the end of 2013.

1. Introduction

Recent seismological studies (e.g., Ross et al., 2020) pointed out that fault zones are complex systems with interacting shear discontinuities (e.g., Fagereng & Sibson, 2010), variable damage volumes (e.g., Powers & Jordan, 2010; Ross et al., 2017), depth-dependent variations in slip behavior, and frictional properties (e.g., Collettini et al., 2011; Shelly et al., 2016). Variations in the tectonic loading (e.g., Frank, 2016; R. Jolivet & Frank, 2020) of different interlaced fault portions, where the frictional properties are rate-strengthening or weakening, can inhibit or promote the nucleation of large earthquakes (e.g., Avouac, 2015). The rate-weakening patches act as locked zones where stress builds up during the interseismic period. In this framework, improved knowledge of the earthquake distribution and interplay between seismic and aseismic parts of the same fault system may help constrain the locked, rate-weakening patches that define seismic potential (e.g., Harris, 2017).

Some extending regions, as the Gulf of Corinth, Apennines, and Southeastern Papua New Guinea, show frequent earthquakes on steep shallow faults and creep on deeper low-angle normal faults (LANFs) (e.g., Abers, 2009; Valoroso et al., 2017; Webber et al., 2018). Even if structures and geological displacements observed in correspondence of outcropping LANFs indicate that they can be tectonically active and accommodate crustal extension (e.g., Collettini & Holdsworth, 2004; Hayman et al., 2003; Hreinsdóttir & Bennett, 2009; John & Foster, 1993; L. Jolivet, Lecomte, et al., 2010; Lister & Davis, 1989; Mirabella et al., 2011; Webber et al., 2018), the frictional properties of these subhorizontal faults, the interplay with shallower faults, and their seismic potential are scarcely known.

The Alto Tiberina Fault (ATF), located in the Northern Apennines within the Umbria-Marche region in central Italy (Figure 1), is an active LANF (e.g., Chiaraluce et al., 2014) within a fold and thrust belt under-

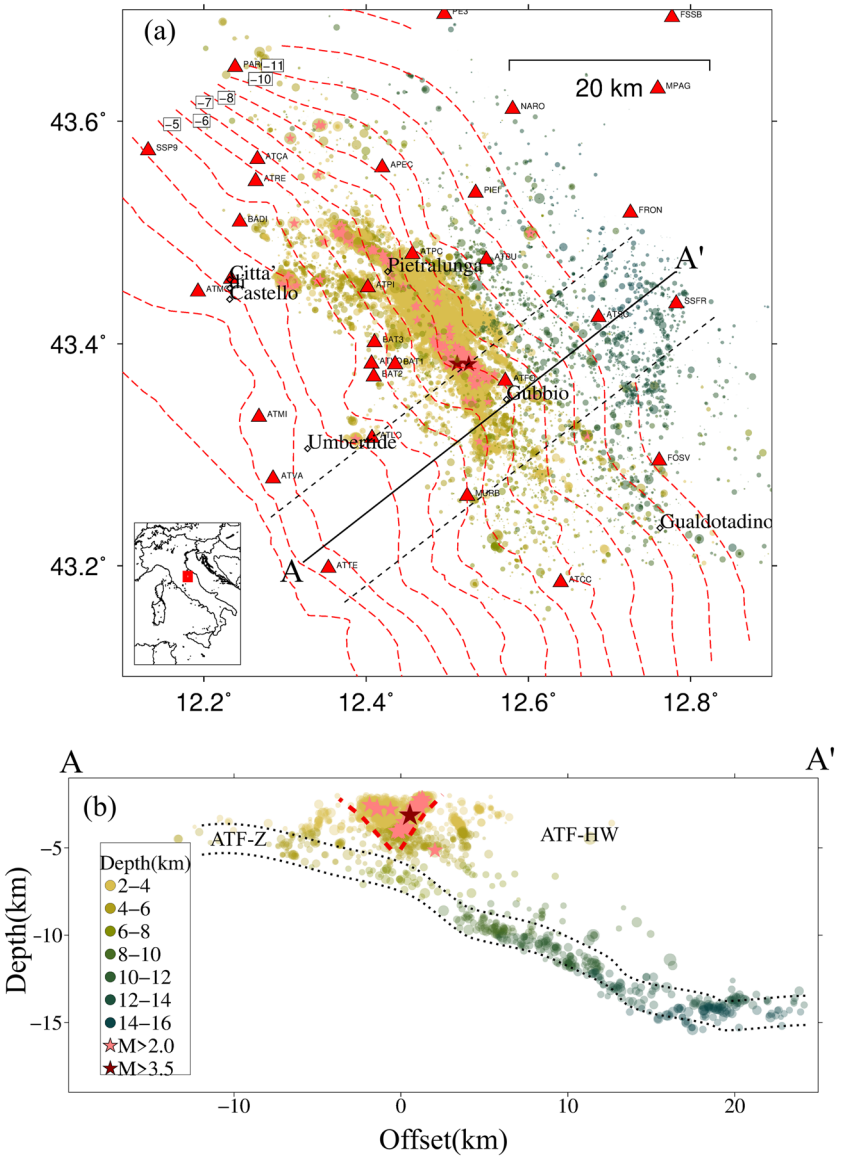

Figure 1. (a) Map of the study area. 33,000 events ($M_L \leq 3.9$) in the hanging-wall volume, and 3,685 events from Valoroso et al. (2017) along the ATF ($M_L \leq 2.4$). Red dashed lines show the isobaths of the ATF projected at surface. Red triangles are seismic stations used, (b) cross section from points A-A′ as shown in (a). Events are colored according to their depth as in the legend. Stars indicate earthquakes with M_L greater than 2 and 3.5, and red dashed lines represent the syn- and antithetic shallower splays.

going NE-trending extension at a rate of about 3 mm/year (Serpelloni et al., 2016). This fault was identified by interpreting deep seismic reflection profiles (Barchi et al., 1998) and by field geology, gravity, magnetic and heat flow data, measurements, and modeling (Boncio et al., 2000; Collettini & Barchi, 2002; Mirabella et al., 2011; Pauselli et al., 2006).

These studies reconstructed a ≈50- to 60-km-long extensional NNW-trending main fault dipping 15–20° from the surface to at least 12–14 km depth, toward ENE. Above the ATF, synthetic and antithetic structures dip at high-angle (40–60°), ending at the intersection with the ATF plane at approximately 3–6 km of depth (Figure 1).

Several geophysical studies investigated ATF mechanical behavior. Vadacca et al. (2016) through a 2-D numerical elastic model including geological and seismic data, simulated the interseismic deformation of the whole fault system. The comparison between the modeling results and GPS data supports the active role

played by ATF in accommodating the ongoing tectonic extension in this sector of the chain. From geodetic data, Gualandi et al. (2017) identified a small aseismic transient signal associated with the occurrence of a shallow sequence lasting about 6 months in 2013–2014 (Gubbio $M_W = 3.8$). The transient produced an extension of about 5 mm with a moment release equivalent to an $M_W = 4.7$, and it was modeled to occur along two minor shallow steeply dipping faults placed within the hanging-wall volume (Figure 1b).

By applying template matching to data collected between 2010 and 2014 (Figure 1), we analyze the ATF seismicity pattern to investigate the mechanical behavior of this LANF. Exploiting a high-resolution earthquake catalog, we investigate the interactions and the possible degree of coupling between the ATF and the shallower system of normal faults. To this end, we characterize the clusters of the augmented catalog in terms of swarms, mainshock-aftershock, and foreshock-mainshock sequences. Including greater detail in the earthquakes patterns and delimiting the fault portions that actively creep or aseismically slip help to better evaluate where stresses accumulate along the ATF and could provide indications on the connection between the fault system heterogeneity and the physics of earthquake initiation.

2. Input Catalog

Instrumental seismicity in the studied area was mainly located in the shallower dipping faults in the ATF hanging-wall and along with the ATF, while the footwall is almost aseismic (Chiaraluce et al., 2007). The high-angle synthetic and antithetic faults in the hanging-wall showed the most energetic sequences in the last 50 years (M_S <5.2 in 1984 Haessler et al., 1988). Small earthquakes along the ATF (M_L <2.4) are released at the average rate of 2.2 events per day (Valoroso et al., 2017) and within ≈1-km-thick dipping fault ranging from ≈3 to 16 km of depth.

The procedure applied by Valoroso et al. (2017) to obtain high-quality locations consisted of using waveform cross-correlation and double-difference methods (Waldhauser & Schaff, 2008). The retrieved catalog contains 36,819 events that occurred between 1 April 2010 and 30 September 2014. Seismic events have at least 12 phase readings, azimuthal gap lower than 180°, residuals (RMS) smaller than 0.3 s, and a formal relative location error of few tens of meters.

The 3-D geometry of the ATF as imaged by seismic reflection profiles (Mirabella et al., 2011) together with relocated seismicity has been used to select events belonging to the ATF and those occurring in its hanging-wall (Figure 1b). The ATF related earthquakes, hereafter named ATF-Z, are the ones nucleating within 1.5 km from the assumed fault surface; these 3,685 events, in the magnitude range $-1 < M_L < 2.4$, represent the input templates.

Under the assumption that the templates widespread along the ATF may represent a meaningful sample in time and space of the fault behavior, we apply a waveform matching technique to detect a more significant number of small earthquakes not yet recognized by conventional techniques. These events contained in the continuous recordings can only be retrieved by the application of a more sensitive and computationally demanding method.

3. Detection Results

By template matching (details in Text S1 in the supporting information and in Sugan et al., 2019; Vuan et al., 2017, 2018), we augment the starting catalog of 16,500 new detections (hereafter named ATF-Z+), most of them having smaller magnitudes than the 3,685 templates, allowing a substantial decrease of completeness magnitude (M_c) from M_L0.6 to less than M_L0.0 (Figure S1). It is worth noting that M_c of the ATF-Z and ATF-Z+ catalogs vary with time during the 5 years decreasing at the end of 2013. This decrease is not due to a different network setting or performance but to rate changes of seismicity. Examples of detection for a template of M_L0.0 finding an M_L0.8 and an M_L-1 event are shown in Figure S2.

Looking at the occurrence of the events versus time in terms of cumulative number, the first novelty unraveled by the new ATF-Z+ catalog is that we do not observe anymore a stable and gradual increase as we did for the templates. Now, the distribution in 5 years time of the new detections in comparison with the hanging-wall seismicity shows (Figure 2) that there is some synchrony in the frequency of occurrence of the events, especially during the moderate shallow sequences at the end of 2013 to early 2014.

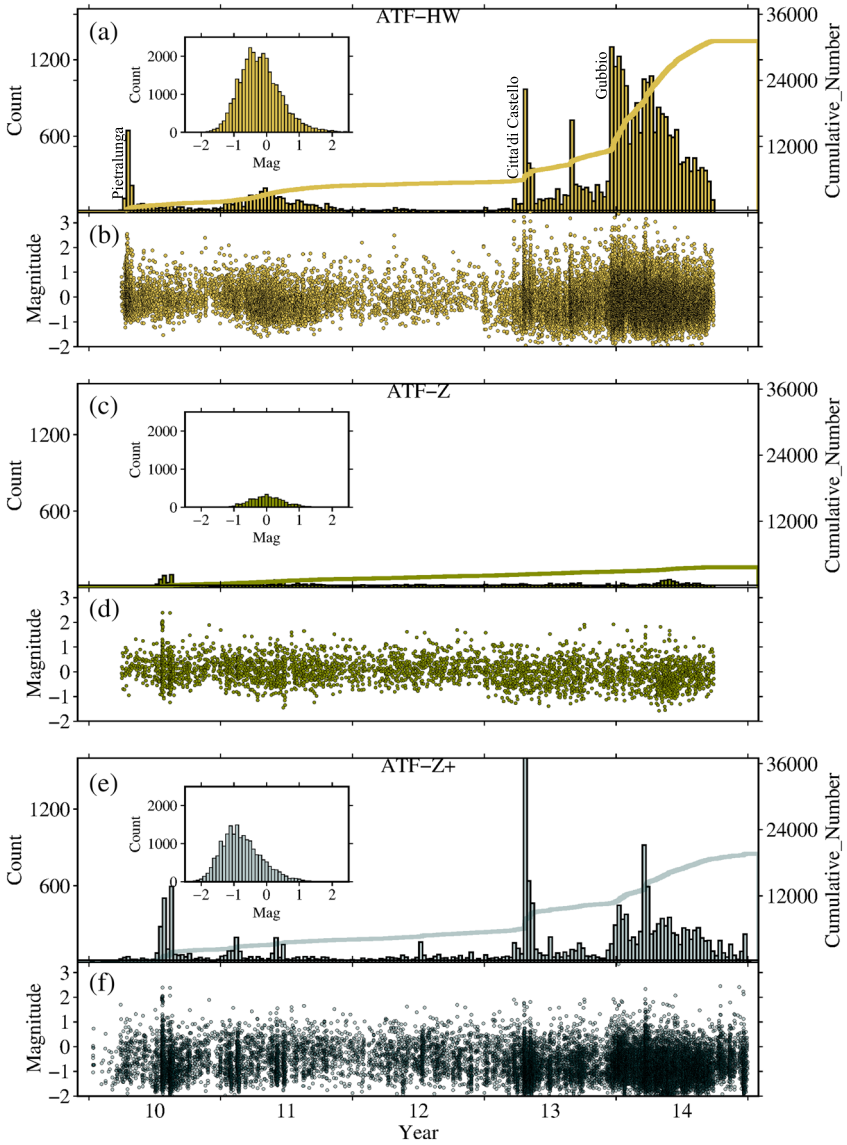

Figure 2. (a) Histograms showing the number of events from 2010 to 2014 in the hanging-wall and (b) time versus magnitude, (c) and (d) as in (a) and (b) for templates catalog, and (e) and (f) for the new augmented catalog. In the inset of (a), (c), and (e) we also show the number of events versus magnitudes. Intermittent bursts are more evident in the augmented than in the templates catalog and generally follow the increase of seismicity in the hanging-wall.

The time-magnitude distribution for the template and ATF-Z+ catalogs are different. The greater detail gained by operating the template matching analysis highlights intermittent bursts spanning the whole period from 2010 to 2014 (Figure 2f), previously completely undetected. Moreover, in ATF-Z+, we are able to fill time windows for which we had no available templates, as in the first months of 2010 or at the end of 2014. We run the waveform matching also for these two unsampled time windows to check both the power of the method and to confirm specific seismicity patterns as the intermittent bursts we find at the end of 2014.

We also detect few new $M_L < 3.0$ events occurring along the ATF in particular when many events happened during the shallower 2013–2014 sequence. Rising seismicity on the hanging-wall often hampers the detection of deeper and lower magnitude ATF earthquakes.

ATF-Z+ samples the fault volume more densely than original ATF-Z (Figure 3). The number of events in ATF-Z+ is considerably increased, and new detections are distributed more homogeneously in the 70 km along-strike area, also showing many clusters.

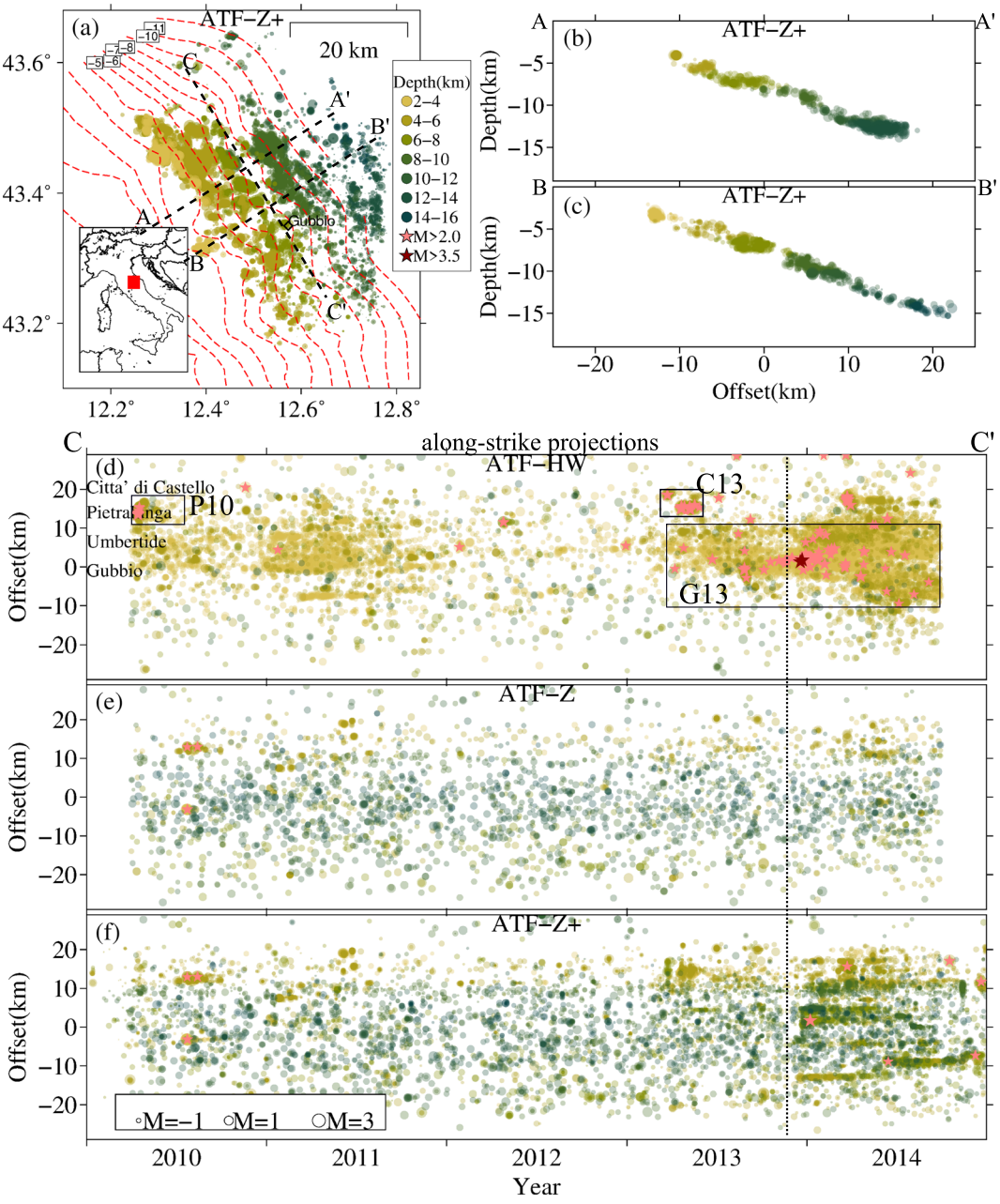

Figure 3. (a) Events from the augmented catalog in map. (b) and (c) Cross-sections along the ATF. (d), (e), and (f) along-strike projections (C-C' in map) of the seismic events in the hanging-wall, for the templates, and augmented catalogs, respectively. Red dashed lines in (a) show the isobaths of the ATF plane projected at surface. The along-strike offset at 0 km corresponds to the first M > 3.0 event of the December 2013 Gubbio sequence. The dotted vertical line indicates the time of increased seismicity in a 30-km-long segment of the ATF-Z+. Rectangles in panel (d) include the Pietralunga 2010 (P10), Cittá di Castello 2013 (C13), and Gubbio 2013–2014 (G13) sequences.

From Figure 3, it is noteworthy the increase of seismicity on ATF after December 2013, spanning an area that extends 30 km along-strike beyond the fault portions activated in the hanging-wall. We also find clusters on ATF portions not included in the templates catalog occurring respectively after or in synchronous with sequences on the shallower splays of the hanging-wall. The distribution of the events at depth indicates some preferential ranges separated by a 1- to 1.5-km-thick layer, from approximately 7–8 km to 8–9 km (see Figure 3a), where seismicity considerably decreases. The decrease of seismic events at ≈8 km of depth (Latorre et al., 2016) seems to coincide with lithological changes (from acoustic to crystalline basement) and an increase in seismic velocities at depth.

4. Interaction Between ATF and Hanging-Wall Splays

The high-resolution catalog we generated represents an exceptional opportunity to correlate the tectonic loading variations, in terms of seismicity rate changes, to the degree of interconnection between different fault segments with varying frictional properties. Hereafter we describe the seismicity pattern of the ATF augmented catalog relative to the seismic sequences occurred along the secondary splays faults located in the hanging-wall, all with multiple mainshocks ranging from $3.0 \leq M_W \leq 3.8$. The primary sequences, extensively described by Valoroso et al. (2017) and Marzorati et al. (2014), occurred in 2010 (Pietralunga, M_W3.6), 2013 (Cittá di Castello, $M_W > 3$) and the long-lasting 2013–2014 (Gubbio, M_W3.8; Figures 1 and 3 for map view and along-strike position, respectively).

Looking at the interplay of the seismic activity within the fault system during the hanging-wall sequence of April–May 2010 (Pietralunga), we do not observe a microseismicity rate increase on the ATF before or immediately after it. Multiple events, starting from July until the end of August 2010, are instead found by template matching on the ATF volume, south of the Pietralunga sequence, as a possible delayed response (Figure 2).

Conversely, during the April 2013 (Cittá di Castello) hanging-wall sequence, we find many undetected events supposed to be related to the ATF (≈2,000) (Figure 3f). The earthquakes along the ATF are almost synchronous with those on the hanging-wall. This sequence is the shallowest one, and the ATF low-angle plane could be, based on this newly discovered seismicity, interconnected with the high-angle normal faults close to Cittá di Castello.

Such a simultaneous activity is also observed during the 2013–2014 Gubbio sequence when the rate change in the ATF affects a ≈30-km-long fault segment (box in Figure 3f). Moreover, along the ATF activated zone, there are particular areas (e.g., strands) of the fault plane where the seismic activity persists over time interspersed with more quiet zones (Figure 3f). The seismic activation of the ATF started in December 2013 and extended slightly beyond the length of the Gubbio fault system. The microseismicity persisted for months after the $M_W > 3$ seismic events between December 2013 and February 2014, suggesting a strong coupling between the system of splay faults in the hanging-wall and the ATF (Figure 3).

If the ATF and the system of splay faults are strongly coupled, we could consider the microseismicity at depth on the ATF as a tracer of a possible afterslip involving an area of ≈250–300 km^2. The same coupling is not observed in the period 2010–2011 and during the first 6 months of 2013 when the same portions of the hanging-wall volume close to Gubbio were active (Figure 3). Therefore, we suggest that the interchange of accelerated microseismicity (end of 2013) could be related to a transient causing a tectonic loading variation on large ATF portions.

5. Clustering Analysis

To further investigate the seismicity pattern and its correlation to tectonic loading variations, we analyze the clustering over time and space (see Text S2). The time-space (T-R) rescaled distribution of the events in ATF-Z+, by applying the Zaliapin and Ben-Zion (2016) approach, helps in separating the clusters from the background seismicity that spans homogeneously all along the ATF with a smooth increase from December 2013 (Figures S3a and S3b).

The clusters, at least for the first couple of years (2010–2012), seem almost homogeneously distributed in space and time mainly in the northern portion of the fault plane (from −10 to 20 km along-strike in Figure S4a). Then, from the end of 2013, contemporaneously to the seismic activity occurred in the splays located north of the Gubbio area, the clusters occurrence increases together with the energy released along a ≈30-km-long fault portion.

In detail, we observe that until December 2013, clusters last no more than a few days and are located all along the fault plane (between 6 and 12 km of depth in Figure S4a). At the end of 2013 until the first few months of 2014, the clusters extend overtime lasting for 2–3 months and appearing as seismic strands in a 30 km along-strike fault segment. Clusters depth is generally shallower (<6 km) in the northern area of the ATF and deepening (6–10 km) in the central part. The same depth distribution of events, more superficial at the edges and deeper in the central zone of the fault, is also shown by the background seismicity (Figure S4b).

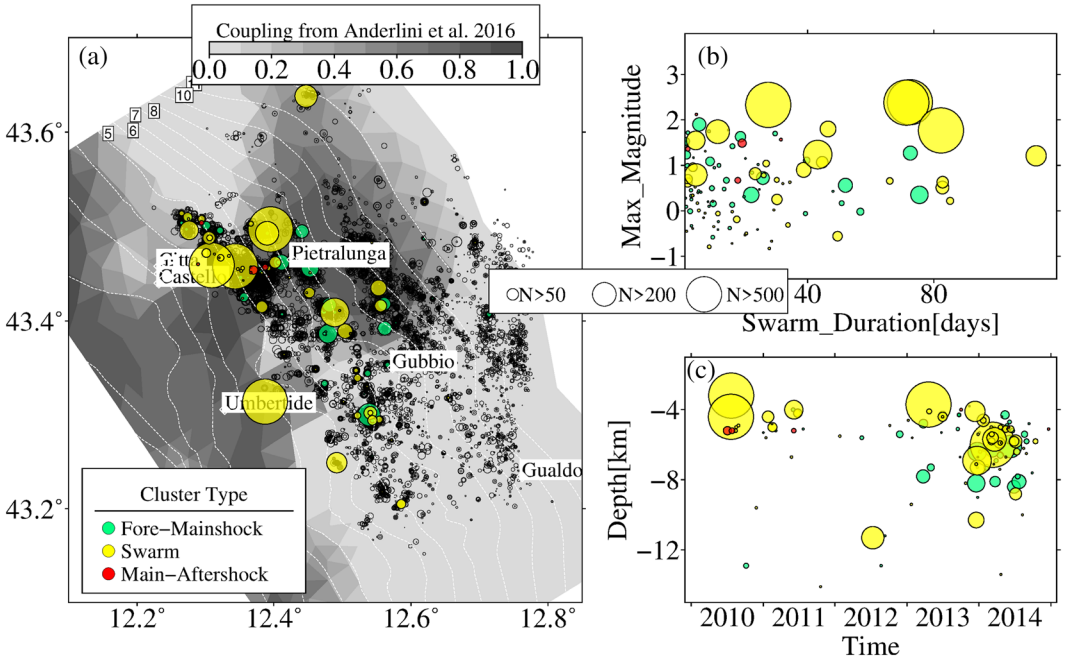

Figure 4. (a) Cluster locations, and in background the coupling of the ATF from Anderlini et al. (2016), (b) cluster duration (days) versus maximum magnitude, (c) cluster time versus depth. Most of the clusters are located in patches close to highly coupled fault regions at depths ranging from 3.5 to 8 km. Swarms (yellow circles) last in the range from few hours to less than 90 days.

The synchronous activation of long-lasting clusters in an area of ≈250–300 km^2 suggests an increasing slip on the ATF since December 2013 and a not negligible role of ATF in the evolution of the aseismic transient observed by Gualandi et al. (2017).

We then classified the clusters in swarms, mainshock-aftershock, and foreshock-mainshock sequences following the criterion proposed by Ogata and Katsura (2012). In Figure S5, we show examples of these types of clusters. The declustering procedure applied to the ATF-Z+ finds 133 clusters with at least 10 events. Forty-eight percent of clusters are classified as foreshock-mainshock, 47% as swarm-like, and only 5% represents typical mainshock-aftershock sequences (Figure 4). Examining the magnitude distribution within each ATF cluster with more than 10 events allow us to understand their development in time and space better. Swarms, more sensitive to changes of the tectonic loading (e.g., Passarelli et al., 2018; Shelly et al., 2016; Toda et al., 2002), persist over time compared with typical foreshock sequences and are characterized by a significantly higher number of events. Few clusters classified as swarms revealed a complex mixed behavior with bursts repetitions in a few days.

6. Discussion

A recent analysis of the ATF seismicity (Valoroso et al., 2017) proposed that the release of small events was constant all along the main fault and widespread, without any evident change in the rate of earthquakes occurrence or evidence for long-lasting clusters. In particular, similarly to Chiaraluce et al. (2007), clusters were considered to be composed of few events (mainly doublets) and having a short duration (hours-day).

The new augmented catalog we obtained, having a greater detail, shows different peculiarities with repeated variations in the seismic release both in space and time. These sudden variations often coincide with moderate seismic sequences (e.g., Cittá di Castello 2013 and Gubbio 2013–2014) activating the shallower splays in the fault hanging-wall; other times the rate changes are instead uncorrelated (e.g., Pietralunga 2010 and some clusters in 2011). Despite in some cases the activation of specific ATF portions is then evident, and coincident with the strongest earthquakes ($M_L > 3.5$) occurring in the structures above, the interaction between the master and secondary faults is challenging to interpret by using only seismic data.

However, we suggest an active role of the leading low angle fault during the occurrence of the slow slip event at the end of 2013. The stress load from the aseismic transient may have induced the ATF rise in seismicity or have been taken place along with the ATF itself. In both cases, the ATF seismic energy release is not enough to fill the gap between the geodetic and the seismic moment. As observed by Gualandi et al. (2017), the seismic moment associated with aseismic slip is, in fact, more than 2 times higher than the value related to the seismic one, and the additional events now included in the ATF-Z+ catalog are still not enough.

Looking at the normalized cumulative seismic moment release with time for the hanging-wall and the ATF-Z+ catalogs, we observe that within the periods when significant shallow sequences above the ATF are absent, the percentage moment growth is 3 times higher in the ATF than in the hanging-wall (Figure S6). As proposed by Anderlini et al. (2016) and Vadacca et al. (2016), we suggest that positive stress accumulation due to ATF creep is most likely released by more favorable oriented shallow splay faults in the hanging-wall ($M_W > 3$ sequences), whose rupture may propagate downdip to the ATF intersection.

The majority of the clusters occurring during the 2013–2014 Gubbio sequence were swarms and foreshock-mainshock sequences, suggesting a combined effect of relaxation and tectonic load that could also be facilitated by the presence of fluids. High pore pressure can induce aseismic creep (e.g., Guglielmi et al., 2015; Wei et al., 2015), and we know about the presence of high CO_2 pressure in ATF footwall observed in kilometers deep boreholes (Collettini & Barchi, 2002; Chiodini et al., 2004). Another signature of the possible combination of tectonic effects with fluids is the presence of fault seismic strands (Figure 3) interspersed with aseismic zones we observe with the new catalog. These structures could represent small patches of velocity weakening material embedded within primarily velocity strengthening material (e.g., Collettini, 2011; Ross et al., 2020; Schwartz & Rokosky, 2007). The spatial distribution of velocity weakening and velocity strengthening patches on the fault interface (e.g., Hetland & Simons, 2010) is linked to the interseismic coupling, and thermal pressurization may control the slip velocity (e.g., Wibberley & Shimamoto, 2005).

At a larger scale, the presence of ATF portions possessing various frictional properties and then possibly corresponding to sectors undergoing seismic or aseismic deformation has been investigated by Anderlini et al. (2016), based on the mapping of the coefficient of interseismic coupling (ratio of long-term seismic slip rate to the tectonic slip rate) and by inverting GPS data (see map in Figure 4a). Surface deformation observations show that, in the interseismic phase between strong earthquakes, some areas remain locked, and others creep aseismically (e.g., Kaneko et al., 2010). The value of coupling depends on the number, size, and spacing of velocity weakening asperities. Anderlini et al. (2016) found that about half of the ATF surface below 5 km of depth is characterized by creep (e.g., low coupling), absorbing a large part of the regional long-term slip rate (1.7 mm/year), while the remaining portions are locked and then able of generating $M > 6$ earthquakes. Following Valoroso et al. (2017), we superposed the 2010–2014 ATF-Z+ seismicity to the map of the coupling proposed by Anderlini et al. (2016) and confirm that the creeping regions (low coupling coefficient) are surrounded by clusters and high seismic activity, while the less productive portions are supposed to be locked (Figure 4a).

We also added to the map the typology of clusters, and we observed that the highest number of events is within swarms. The location at the edges of higher coupling patches is confirmed for almost all clusters regardless of their classification and is also reflected in the location of the repeaters highlighted by Valoroso et al. (2017) on the ATF. Figures 4b and 4c also show the cluster type in relation to their maximum magnitude, depth, and duration. Swarms duration (0–120 days) generally increases with the maximum magnitude, and depths range from 3 to 8 km.

The observations made on creep and interseismic coupling suggest some mechanical implications. First, from the microseismicity pattern analysis, we confirm that a mixed distribution of locked and creeping patches seems to characterize the ATF. Second, the ATF is a thick fault zone in which heterogeneous rocks accommodate seismic-aseismic shear slip with different frictional properties. Third, since the ATF also shows a high degree of tectonic coupling with its main antithetic faults, it is likely that microseismicity and aseismic slip on ATF may control the seismic activity on the shallower splays. This ATF specific behavior can be retrieved in other tectonic environments (e.g., Harris, 2017), in laboratory experiments (e.g., Collettini et al., 2011) and in numerical simulations (e.g., van den Ende et al., 2020) and confirm the recent evidence about the control of seismicity by complex fault systems (e.g., Ross et al., 2020). A better understanding of the interplay of the seismic activity within complex fault systems, including segments undergoing both

creeping and fast/slow slip earthquakes, seems to be the main road to provide better earthquake hazard characterizations (e.g., Avouac, 2015; Bürgmann, 2018).

7. Conclusions

The ATF is a creeping low-angle normal fault (15–20°) characterized by frequent moderate earthquakes on steeply dipping, shallow secondary faults. From 2010 to 2014, by using a template matching approach, we obtain a fivefold increase in ATF earthquake detections and a decrease of ≈0.5–0.7 of the completeness magnitude. We identify previously hidden features such as the variation of the rate of occurrence of the seismicity along the ATF, including the presence of at least 133 highly productive (more than 10 events) clusters. The majority of clusters behave as fore-mainshock sequences (48%) and swarms (47%); sometimes lasting more than 40 days. Clusters occur around fault patches with a low seismicity rate and higher coupling between the shallow crust and the ATF. Looking at the seismic behavior of ATF in relation with sequences occurring in the high-angle normal faults at shallow depth, we show that the ATF is mainly active at variable intermittent rates and interplaying with moderate earthquakes in the hanging-wall. This intermittency is evident along-strike for fault strands that extend below and at the edges of the shallower faults. As an example, we observe that the ATF shows a rise in the seismic activity during the occurrence of the slow slip associated with the 2013–2014 sequence.

Data Availability Statement

INGV manages the TABOO stations (Chiaraluce et al., 2014) - Seismological Data Centre (https://doi.org/10.13127/SD/X0FXNH7QFY), and data to support this article are available via EIDA (the European Integrated Data Archive infrastructure within ORFEUS) (http://www.orfeus-eu.org/webdc3/). TABOO is a multidisciplinary geophysical observatory of INGV, designed for the study of deformation processes active along with a system of extensional faults in the Northern Apennines and for the identification of earthquake preparation processes. Computations are performed at CINECA in the framework of the HPC-TRES program agreement between OGS and CINECA. PyMPA software is freely available online (https://github.com/avuan/PyMPA37). The code development is partially supported by the project Seismology and Earthquake Engineering Research Infrastructure Alliance for Europe (SERA), responding to the priorities identified in the call INFRAIA-01-2016-2017 Research Infrastructure for Earthquake Hazard. Figures were produced using the Generic Mapping Tools version 5.0 (http://gmt.soest.hawaii.edu/ Wessel & Luis, 2017).

Acknowledgments
We thank Ilya Zaliapin for kindly providing the declustering code. We also thank the associate editor Åke Fagereng and two anonymous reviewers for their careful reading, comments, and suggestions that helped to improve the manuscript.

References

Abers, G. A. (2009). Slip on shallow-dipping normal faults. *Geology*, *37*(8), 767–768. https://doi.org/10.1130/focus082009.1

Anderlini, L., Serpelloni, E., & Belardinelli, M. E. (2016). Creep and locking of a low-angle normal fault (2016): Insights from the Altotiberina fault in the Northern Apennines (Italy). *Geophysical Research Letters*, *43*, 4321–4329. https://doi.org/10.1002/2016GL068604

Avouac, J. P. (2015). From geodetic imaging of seismic and aseismic fault slip to dynamic modeling of the seismic cycle. *Annual Review of Earth and Planetary Sciences*, *43*(1), 233–271. https://doi.org/10.1146/annurev-earth-060614-105302

Barchi, M. R., De Feyter, A., Magnani, M. B., Minelli, G., Pialli, G., & Sotera, B. M. (1998). Extensional tectonics in the Northern Apennines (Italy): Evidence from the CROP03 deep seismic reflection line. *Memorie Societá Geologica Italiana*, *52*, 527–538. https://doi.org/10.1029/2004GL022256

Boncio, P., Brozzetti, F., & Lavecchia, G. (2000). Architecture and seismotectonics of a regional low-angle normal fault zone in central Italy. *Tectonics*, *19*, 1038–1055. https://doi.org/10.1029/2000TC900023

Bürgmann, R. (2018). The geophysics, geology and mechanics of slow fault slip. *Earth and Planetary Science Letters*, *495*, 112–134. https://doi.org/10.1016/j.epsl.2018.04.062

Chiaraluce, L., Amato, A., Carannante, S., Castelli, S., Cattaneo, M., Cocco, M., & Valoroso, L. (2014). The Alto Tiberina near fault observatory (Northern Apennines, Italy). *Annales de Geophysique*, *57*, 327. https://doi.org/10.4401/ag

Chiaraluce, L., Chiarabba, C., Collettini, C., Piccinini, D., & Cocco, M. (2007). Architecture and mechanics of an active low-angle normal fault: Alto Tiberina Fault, northern Apennines, Italy. *Journal of Geophysical Research*, *112*, B10310. https://doi.org/10.1029/2007JB005015

Chiodini, G., Cardellini, C., Amato, A., Boschi, E., Caliro, S., Frondini, F., & Ventura, G. (2004). Carbon dioxide earth degassing and seismogenesis in central and southern italy. *Geophysical Research Letters*, *31*, L07615. https://doi.org/10.1029/2004GL019480

Collettini, C. (2011). The mechanical paradox of low angle normal faults: Current understanding and open questions. *Tectonophysics*, *510*, 253–268. https://doi.org/10.1016/j.tecto.2011.07.015

Collettini, C., & Barchi, M. R. (2002). A low angle normal fault in the Umbria region (central Italy): A mechanical model for the related microseismicity. *Tectonophysics*, *359*, 97–115. https://doi.org/10.1016/S0040-1951(02)00441-9

Collettini, C., & Holdsworth, R. E. (2004). Fault zone weakening processes along low-angle normal faults: Insights from the Zuccale Fault, Isle of Elba, Italy. *Journal of the Geological Society London*, *161*, 1039–1051. https://doi.org/10.1144/0016-764903-179

Collettini, C., Niemeijer, A., Viti, C., Smith, S. A. F., & Marone, C. (2011). Fault structure, frictional properties and mixed-mode fault slip behavior. *Earth and Planetary Science Letters*, *311*(3), 316–327. https://doi.org/10.1016/j.epsl.2011.09.020

Fagereng, Å., & Sibson, R. H. (2010). Mlange rheology and seismic style. *Geology*, *38*(8), 751–754. https://doi.org/10.1130/G30868.1
Frank, W. B. (2016). Slow slip hidden in the noise: The intermittence of tectonic release. *Geophysical Research Letters*, *43*, 10,125–10,133. https://doi.org/10.1002/2016GL069537
Gualandi, A., Nichele, C., Serpelloni, E., Chiaraluce, L., Anderlini, L., Latorre, D., et al. (2017). Aseismic deformation associated with an earthquake swarm in the northern Apennines (Italy). *Geophysical Research Letters*, *44*, 7706–7714. https://doi.org/10.1002/2017GL073687
Guglielmi, Y., Cappa, F., Avouac, J. P., Henry, P., & Elsworth, D. (2015). Seismicity triggered by fluid injection induced aseismic slip. *Science*, *348*(6240), 1224–1226. https://doi.org/10.1126/science.aab0476
Haessler, H., Gaulon, R., Rivera, L., Console, R., Frogneux, M., Gasparini, G., et al. (1988). The Perugia (Italy) earthquake of 29. April 1984: A microearthquake survey. *Bulletin of the Seismological Society of America*, *78*, 1948–1964.
Harris, R. A. (2017). Large earthquakes and creeping faults. *Reviews of Geophysics*, *55*, 169–198. https://doi.org/10.1002/2016RG000539
Hayman, N. W., Knott, J. R., Cowan, D. S., Nemser, E., & Sarna-Wojcicki, A. (2003). Quaternary low-angle slip on detachment faults in Death Valley, California. *Geology*, *31*, 343–346. https://doi.org/10.1130/0091-7613(2003)031
Hetland, E. A., & Simons, M. (2010). Post-seismic and interseismic fault creep II: Transient creep and interseismic stress shadows on megathrusts. *Geophysical Journal International*, *181*(1), 99–112. https://doi.org/10.1111/j.1365-246X.2009.04482.x
Hreinsdóttir, S., & Bennett, R. A. (2009). Active aseismic creep on the Alto Tiberina low-angle normal fault, Italy. *Geology*, *37*(8), 683–686. https://doi.org/10.1130/G30194A.1
John, B. E., & Foster, D. A. (1993). Structural and thermal constraints on the initiation angle of detachment faulting in the southern Basin and Range: The Chemehuevi Mountains case study. *Geological Society of America Bulletin*, *105*, 1091–1108. https://doi.org/10.1130/00167606(1993)105
Jolivet, R., & Frank, W. B. (2020). The transient and intermittent nature of slow slip. *AGU Advances Journal*, *1*(1), e2019AV000126. https://doi.org/10.1029/2019AV000126
Jolivet, L., Lecomte, E., Huet, B., Denele, Y., Lacombe, O., Labrousse, L., et al. (2010). The North Cycladic detachment system. *Earth and Planetary Science Letters*, *289*, 87–104. https://doi.org/10.1016/j.epsl.2009.10.032
Kaneko, Y., Avouac, J. P., & Lapusta, N. (2010). Towards inferring earthquake patterns from geodetic observations of interseismic coupling. *Nature Geosciences*, *3*, 363–369. https://doi.org/10.1038/ngeo843
Latorre, D., Mirabella, F., Chiaraluce, L., Trippetta, F., & Lomax, A. (2016). Assessment of earthquake locations in 3D deterministic velocity models: A case study from the Altotiberina Near Fault Observatory (Italy). *Journal of Geophysical Research: Solid Earth*, *121*, 8113–8135. https://doi.org/10.1002/2016JB013170
Lister, G. S., & Davis, G. A. (1989). The origin of metamorphic core complexes and detachment faults formed during Tertiary continental extension in the northern Colorado River region. *USA, Journal of Structural Geology*, *11*, 65–94. https://doi.org/10.1016/0191-8141(89)90036-9
Marzorati, S., Massa, M., Cattaneo, M., Monachesi, G., & Frapiccini, M. (2014). Very detailed seismic pattern and migration inferred from the April 2010 Pietralunga (Northern Italian Apennines) microearthquake sequence. *Tectonophysics*, *610*, 91–109. https://doi.org/10.1016/j.tecto.2013.10.014
Mirabella, F., Brozzetti, F., Lupattelli, A., & Barchi, M. R. (2011). Tectonic evolution of a low angle extensional fault system from restored cross sections in the northern Apennines (Italy). *Tectonics*, *30*, TC6002. https://doi.org/10.1029/2011TC002890
Ogata, Y., & Katsura, K. (2012). Prospective foreshock forecast experiment during the last 17 years. *Geophysical Journal International*, *191*, 1237–1244. https://doi.org/10.1111/j.1365-246X.2012.05645.x
Passarelli, L., Rivalta, E., Jnsson, S., Hensch, M., Metzger, S., Jakobsdttir, S. S., et al. (2018). Scaling and spatial complementarity of tectonic earthquake swarms. *Earth and Planetary Science Letters*, *482*, 62–70. https://doi.org/10.1016/j.epsl.2017.10.052
Pauselli, C., Barchi, M. R., Federico, C., Magnani, M. B., & Minelli, G. (2006). The crustal structure of the Northern Apennines (Central Italy): An insight by the CROP03 seismic line. *American Journal of Science*, *306*, 428–450. https://doi.org/10.2475/06.2006.02
Powers, P. M., & Jordan, T. H. (2010). Distribution of seismicity across strike-slip faults in California. *Journal of Geophysical Research*, *115*, B05305. https://doi.org/10.1029/2008JB006234
Ross, Z. E., Cochran, E. S., Trugman, D. T., & Smith, J. D. (2020). 3D fault architecture controls the dynamism of earthquake swarms. *Science*, *368*(6497), 1357–1361. https://doi.org/10.1126/science.abb0779
Ross, Z. E., Hauksson, E., & Ben-Zion, Y. (2017). Abundant off-fault seismicity and orthogonal structures in the San Jacinto fault zone. *Science Advances*, *3*(3), 1–8.
Schwartz, S. Y., & Rokosky, J. M. (2007). Slow slip events and seismic tremor at circum Pacific subduction zones. *Reviews of Geophysics*, *45*, RG3004. https://doi.org/10.1029/2006RG000208
Serpelloni, E., Vannucci, G., Anderlini, L., & Bennett, R. A. (2016). Kinematics, seismotectonics and seismic potential of the eastern sector of the European Alps from GPS and seismic deformation data. *Tectonophysics*, *688*, 157–181. https://doi.org/10.1016/j.tecto.2016.09.026
Shelly, D. R., Ellsworth, W. L., & Hill, D. P. (2016). Fluid-faulting evolution in high definition: Connecting fault structure and frequency-magnitude variations during the 2014 Long Valley Caldera, California, earthquake swarm. *Journal of Geophysical Research: Solid Earth*, *121*, 1776–1795. https://doi.org/10.1002/2015JB012719
Sugan, M., Vuan, A., Kato, A., Massa, M., & Amati, G. (2019). Seismic evidence of an early afterslip during the 2012 sequence in Emilia (Italy). *Geophysical Research Letters*, *46*, 625–635. https://doi.org/10.1029/2018GL079617
Toda, S., Stein, R. S., & Sagiya, T. (2002). Evidence from the ad 2000 Izu islands earthquake swarm that stressing rate governs seismicity. *Nature*, *418*, 58–61. https://doi.org/10.1038/nature00997
Vadacca, L., Casarotti, E., Chiaraluce, L., & Cocco, M. (2016). On the mechanical behaviour of a low-angle normal fault: The Alto Tiberina fault (Northern Apennines, Italy) system case study. *Solid Earth*, *7*(6), 1537–1549. https://doi.org/10.5194/se-7-1537-2016
Valoroso, L., Chiaraluce, L., Di Stefano, R., & Monachesi, G. (2017). Mixed-mode slip behaviour of the Altotiberina low-angle normal fault system (Northern Apennines, Italy) through high-resolution earthquake locations and repeating events. *Journal of Geophysical Research: Solid Earth*, *122*, 10,220–10,240. https://doi.org/10.1002/2017JB014607
van den Ende, M. P. A., Chen, J., Niemeijer, A. R., & Ampuero, J.-P. (2020). Rheological transitions facilitate fault-spanning ruptures on seismically active and creeping faults. *Journal of Geophysical Research: Solid Earth*, *125*, e2019JB019328. https://doi.org/10.1029/2019JB019328
Vuan, A., Sugan, M., Amati, G., & Kato, A. (2018). Improving the detection of low-magnitude seismicity: Development and optimization of a scalable code based on the cross-correlation of template earthquakes. *Bulletin of the Seismological Society of America*, *108*(1), 471–480. https://doi.org/10.1785/0120170106
Vuan, A., Sugan, M., Chiaraluce, L., & Di Stefano, R. (2017). Loading rate variations along a mid-crustal shear zone preceding the Mw 6.0 earthquake of 24 August 2016 in Central Italy. *Geophysical Research Letters*, *44*, 12,170–12,180. https://doi.org/10.1002/2017GL076223

Waldhauser, F., & Schaff, D. P. (2008). Large scale relocation of two decades of Northern California seismicity using cross correlation and double difference methods. *Journal of Geophysical Research*, *113*, B08311. https://doi.org/10.1029/2007JB005479
Webber, S., Norton, K. P., Little, T. A., Wallace, L. M., & Ellis, S. (2018). How fast can low-angle normal faults slip? Insights from cosmogenic exposure dating of the active Mai iu fault, Papua New Guinea. *Geology*, *46*(3), 227–230. https://doi.org/10.1130/G39736.1
Wei, S., Avouac, J. P., Hudnut, K. W., Donnellan, A., Parker, J. W., Graves, R. W., et al. (2015). The 2012 Brawley swarm triggered by injection-induced aseismic slip. *Earth and Planetary Science Letters*, *422*, 115–125. https://doi.org/10.1016/j.epsl.2015.03.054
Wessel, P., & Luis, J. F. (2017). The GMT/MATLAB toolbox. *Geochemistry, Geophysics, Geosystems*, *18*, 811–823. https://doi.org/10.1002/2016GC006723
Wibberley, C. A., & Shimamoto, T. (2005). Earthquake slip weakening and asperities explained by thermal pressurization. *Nature*, *436*, 689–692. https://doi.org/10.1038/nature03901
Zaliapin, I., & Ben-Zion, Y. (2016). A global classification and characterization of earthquake clusters. *Geophysical Journal International*, *207*(1,1), 608–634. https://doi.org/10.1093/gji/ggw300

References From the Supporting Information

Baillard, C., Crawford, W. C., Ballu, V., Hibert, C., & Mangeney, A. (2014). An automatic Kurtosis based P- and S-phase picker designed for local seismic networks. *Bulletin of the Seismological Society of America*, *104*(1), 394–409. https://doi.org/10.1785/0120120347
Cao, A. M., & Gao, S. S. (2002). Temporal variations of seismic b?values beneath northeastern japan island arc. *Geophysical Research Letters*, *29*(9), 1334. https://doi.org/10.1029/2001GL013775
Chiaraluce, L., Collettini, C., Cattaneo, M., & Monachesi, G. (2014). The shallow boreholes at the Altotiberina near fault Observatory (TABOO; northern Apennines of Italy). *Scientific Drilling*, *17*, 31–35. https://doi.org/10.5194/sd
Crotwell, H. P., Owens, T. J., & Ritsema, J. (1999). The TauP Toolkit: Flexible seismic travel-time and ray-path utilities. *Seismological Research Letters*, *70*, 154–160. https://doi.org/10.1785/gssrl.70.2.154
Kato, A., Obara, K., Igarashi, T., Tsuruoka, H., Nakagawa, S., & Hirata, N. (2012). Propagation of slow slip leading up to the 2011 Mw 9.0 Tohoku-Oki Earthquake. *Science*, *335*, 705–708. https://doi.org/10.1126/science.1215141
Krischer, L., Megies, T., Barsch, R., Beyreuther, M., Lecocq, T., Caudron, C., & Wassermann, J. (2015). ObsPy: A bridge for seismology into the scientific Python ecosystem. *Computational Science & Discovery*, *8*(1), 014003. https://doi.org/10.1088/1749-4699/8/1/014003
Kwiatek, G., & Ben-Zion, Y. (2016). Theoretical limits on detection and analysis of small earthquakes. *Journal of Geophysical Research: Solid Earth*, *121*. https://doi.org/10.1002/2016JB012908
Munafò, I., Malagnini, L., & Chiaraluce, L. (2016). On the relationship between Mw and ML for Small Earthquakes. *Bulletin of the Seismological Society of America*, *106*, 2402–2408. https://doi.org/10.1785/0120160130
Shelly, D. R., Beroza, G. C., & Ide, S. (2007). Non-volcanic tremor and low-frequency earthquake swarms. *Nature*, *446*, 305–307. https://doi.org/10.1038/nature05666
Sugan, M., Kato, A., Miyake, H., Nakagawa, S., & Vuan, A. (2014). The preparatory phase of the 2009 Mw 6.3 L'Aquila earthquake by improving the detection capability of low-magnitude foreshocks. *Geophysical Research Letters*, *41*, 6137–6144. https://doi.org/10.1002/2014GL061199
Zaliapin, I., & Ben-Zion, Y. (2020). Earthquake declustering using the nearest-neighbor approach in space-time-magnitude domain. *Journal of Geophysical Research: Solid Earth*, *125*(4), e2018JB017120. https://doi.org/10.1029/2018JB017120
Zhang, M., & Wen, L. (2015). An effective method for small event detection: Match and locate. *Geophysical Journal International*, *200*, 1523–1537. https://doi.org/10.1093/gji/ggu466